

The mechanisms of debris flow: a preliminary study

Les mécanismes de l'écoulement de débris: une étude préliminaire

G.D. Zhou, R.P.H. Law & C.W.W. Ng

Department of Civil and Environmental Engineering, Hong Kong University of Science and Technology, HKSAR

ABSTRACT

Due to its complexity, the fundamental mechanism of debris flow is still not fully understood. In this study, debris flow mobility and reverse segregation were investigated experimentally. A 1.4 m long flume inclining at an angle of 45° to the horizontal and a 4.4 m long flume were used to study mobility and reverse segregation, respectively. Leighton Buzzard sands (fractions C & E) (uniform sands) and completely decomposed granite (CDG, a non-uniform sandy soil) prepared at different water contents were used to simulate different debris flows in the experiments. With the use of a high-speed camera, particle trajectories in dry granular flows were captured. The mechanism of reverse segregation during the deposition process was investigated.

RÉSUMÉ

En raison de sa complexité, le mécanisme fondamental de l'écoulement de débris toujours entièrement n'est pas compris. Dans cette étude, la mobilité d'écoulement de débris et la ségrégation renversée ont été étudiées expérimentalement. Un 1.4 m longue ravin inclinant sous un angle de 45° à l'horizontale et un 4.4 m longue ravin ont été employées pour étudier la mobilité et la ségrégation renversée, respectivement. Sables de Leighton Buzzard (fractions C et E) (sables uniformes) et granite complètement décomposé (CDG, un sol sableux non-uniforme) préparé à différentes teneurs en eau ont été employés pour simuler différents écoulements de débris dans les expériences. Avec l'utilisation d'une caméra à grande vitesse, la trajectoire de particules dans des écoulements granulaires secs ont été capturées. Le mécanisme de la ségrégation renversée pendant le procédé de déposition a été étudié.

Keywords : flume model test, debris flow mobility, reverse segregation

1 INTRODUCTION

Debris flows and avalanches consist of multiple mixtures of solids, sand, gravel, rocks, ice, snow, and water that move down slopes under the driving force of gravity (Hunt 1994). The high flowing velocity, large impact forces, and long run-out distance, combined with poor temporal predictability, cause debris flows and debris avalanches to be one of the most hazardous types of landslide (Jakob & Hungr 2005). Thus, it is necessary to analyze the fundamental mechanisms of debris flows and to predict when such disasters will occur if possible.

According to Lo (2000), the run-out distance of a landslide is usually considered through assessment of the damage consequences. To study the mobility of different landslides systematically, the energy line concept was applied and a travel angle was defined (Cruden & Varnes 1996). The travel angle is measured from the crest of the scarp to the distal end of the debris. This concept is simple and appropriate in risk assessments.

As Rombi et al. (2006) pointed out, debris flow behaviour is affected by a number of variables such as the moisture content, grain size distribution and overall volume of the soil. Rombi et al.'s physical model tests showed that an increased water content could result in a long run-out distance. Also, previous studies on the effects of flow volume on the travel angle revealed the trend that an increase in the volume generally resulted in a reduction in the travel angle (Davies 1982). However, these empirical observations should be investigated systematically.

Based on field observations and experimental tests (Takahashi 1991, Major 1997), a key conclusion was drawn that in saturated debris flows, segregation is observed between deposited layers. Coarse particles accumulate in the front and on the top surface while fine particles move downward and to the

rear of the flow. In dry granular debris flows, the influence of longitudinal segregation (along the flowing direction) on the front velocity was preliminarily studied by Law et al. (2007). However, in the deposition zone, detailed descriptions of particle interactions before a rigid barrier and convincing explanations for the reverse segregation along the flow height are still not available.

This study investigates debris flow mobility using a 1.4 m long flume model. Leighton Buzzard (LB) sands (fractions C & E) and completely decomposed granite (CDG) were used in the experimental tests. Emphasis was placed on the effects of the water content, the total debris mass and the grain size on the travel angle.

In addition, a 4.4 m long flume model was used to investigate reverse segregation mechanisms along the flow height. Particle movements were captured by a high-speed camera. Emphasis was placed on the reverse segregation that occurred in the deposition zone.

2 DETAILS OF FLUME MODEL TESTS

2.1 *Experimental setup for the mobility study*

Figure 1 shows the 1.4 m long flume model for studying the mobility of debris flows. It consisted of a transportation zone and a deposition zone. The transportation zone was an inclined slope channel that was 1.4 m long and 0.4 m wide. The slope angle was fixed at 45°. The deposition zone was a flat channel that was 1.2 m long and 0.4 m wide. Both the transportation zone and the deposition zone were made smooth by self-adhesive plastic sheets to ensure uniform roughness. The flume model was mainly made of plywood, with a Perspex window cut into one side, at which the video camera was installed to

view the flow behaviour. The materials to be tested were placed in a hopper at the top of the slope. The prepared granular materials were placed in the hopper just before each test started to minimize possible consolidation and segregation. A pneumatically operated trapdoor to the hopper was used to control the release of the granular material onto the slope channel.

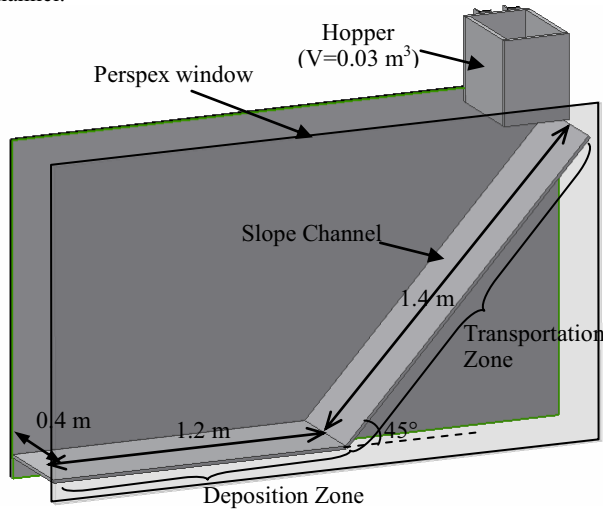


Figure 1. Experimental setup of the 1.4 m long flume model

2.2 Experimental setup for the study on reverse segregation

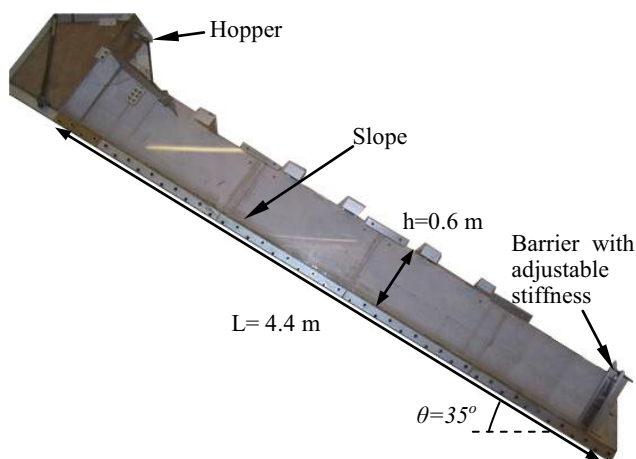


Figure 2. Experimental setup of 4.4 m long flume model

In order to study segregation of debris flow along the travelling process and in the deposition zone, a long channel slope was used with an impact barrier (see Figure 2). The model dimensions of the flume were 4.4 m long, 0.4 m wide and 0.6 m deep. The slope angle was adjusted to be 35° and the slope surface was made smooth by self-adhesive plastic sheets. The flume was mainly made of plywood, with a Perspex window cut into one side at which a high-speed camera was installed to view the flow behaviour. An aluminium stopping plate was installed as an impact barrier. A pneumatically operated trapdoor to the hopper was linked electronically to record the time-zero for the flow tests.

During the tests, the high-speed camera was focused on the deposition zones to capture the trajectories of the particles and record sequences of images from 60 to 8000 frames per second under a certain limited image memory. When the recording rate was set to 250 frames per second, the complete impact behaviour of the debris mass could be recorded and the resolution was kept suitable for analysis.

2.3 Test plan and procedures

The debris flow simulations started with the release of the granular material in the hopper. To study debris flow mobility, flume tests were conducted in three series. Firstly, the influence of water content on the granular materials with different mean particle sizes and different particle size distributions was studied. Uniform sands (LB sands) and CDG (with non-uniform particles) were released into the channel to simulate the granular flows. Figure 3 shows the particle size distributions of the LB sands (fractions C & E) and CDG used in the tests. The water content of the soil sample was varied at 0%, 15%, 20%, 25% and 30%, while the total soil mass was kept constant and equal to 5 kg. Secondly, the effect of the granular mass on the flow mobility was investigated. Dry LB sands (fractions C & E) and CDG were released individually while the total soil mass was varied at 2 kg, 4 kg, 8 kg, 16 kg and 24 kg. Thirdly, the effects of fine particles in dry granular flows were studied. Mixtures of LB sand (fraction C) with fine sand (fraction E) were released. The percentage of LB sand (fraction E) in the mixture was varied at 0%, 30%, 50%, 70% and 100% while the total mass of the mixtures was kept at 10 kg. The test plans of the flume model tests described above are summarized in Table 1.

To investigate the mechanism of reverse segregation, thirty kg of dry CDG was released into the smooth 4.4 m flume channel. The flow characteristics of non-uniform particles were examined with the aid of using a high-speed camera.

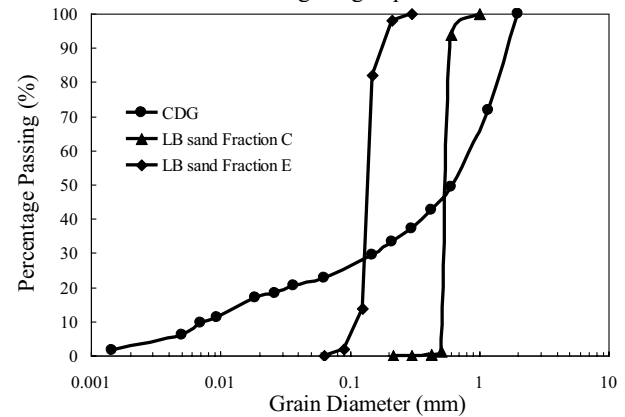


Figure 3. Particle size distributions of LB sands (fractions C & E) and CDG

Table 1. Test plan of the flume model tests.

Series	Material	Water Content (%)	Mass (kg)	
1	LB sands (fraction C & E) and CDG	0/15/20/25/30	5	
2	LB sands (fraction C & E) and CDG	0	2/4/8/16/24	
3	LB sand fraction C (%)	LB sand fraction E (%)	Water Content (%)	Mass (kg)
	100	0	0	10
	70	30	0	10
	50	50	0	10
	30	70	0	10
	0	100	0	10

3 INTERPRETATION OF TEST RESULTS

3.1 Investigation of debris flow mobility

3.1.1 The effects of water content on flow mobility

Figure 4 compares the measured travel angles of CDG and LB sands (fractions C & E) mixed with different water contents.

The measured travel angle of LB sand (fraction C) increases from 32° to around 41° when the water content is increased from 0% to 20%. However, the travel angle decreases when the water content is increased beyond 20%. A similar trend is observed for CDG, although the water content corresponding to the largest travel angle (smallest run-out distance) is 25%. By using much finer particles (fraction E sand), increasing the water content beyond 30% does not increase the run-out distance as most of the sand perches on the slope. The mechanism remains to be further elucidated.

It is expected that the mobility of unsaturated debris flows should be governed by the unsaturated shear strength (resistance acting on the slope bed). For simplicity, the shear strength of unsaturated soils may be related to the water content and the matric suction (Vanapalli et al. 1996; Ng & Menzies 2007) as follows:

$$\tau = [c' + (\sigma_n - u_a) \tan \phi'] + (u_a - u_w)[(\Theta^\kappa)(\tan \phi')], \quad (1)$$

where $(u_a - u_w)$ is the matric suction, Θ is the normalized volumetric water content, κ is a fitting parameter, ϕ' is the effective friction angle and c' is the effective cohesion.

The peak travel angles in Figure 4 reveal the existence of a maximum resistance to flowing materials for some soils and they may be explained as follows. Although the matric suction is reduced with a small increase in the water content from a dry condition (high suction) in sands and CDG, the soil-water contact area is increased as the normalized volumetric water content, Θ , is increased. The coupled effects, $(u_a - u_w)\Theta^\kappa$, increase the shear strength, τ , and reduce the debris flow mobility (the travel angle is increased). With a further increase in the water content to the saturated condition, the matric suction is destroyed ($u_a - u_w = 0$) and the flow resistance, τ , is reduced to the minimum. In addition, high pore pressures in saturated debris flows help to sustain debris mobility (Iverson 1997). Thus, reduced travel angles occur with high water contents and inflections (critical water contents) are observed on the curves.

Figure 4 also reveals that granular materials with different mean particle sizes have different critical water contents. A reasonable explanation is that during slope failure and sliding, the pore water pressure is affected by the permeability of the soil (Wang and Sassa 2003). The lower the permeability, the lower the dissipation rate of the pore pressure. In unsaturated debris flows, the lower permeability means that the matric suction is sustained and there is a higher resistance to flow. Experimental results show that the smaller the mean particle diameter, d_{50} (LB sand fraction E), the larger the water content. Soils with non-uniform particle size distributions (CDG) have a higher critical water content than do uniform soils (LB sand fraction C).

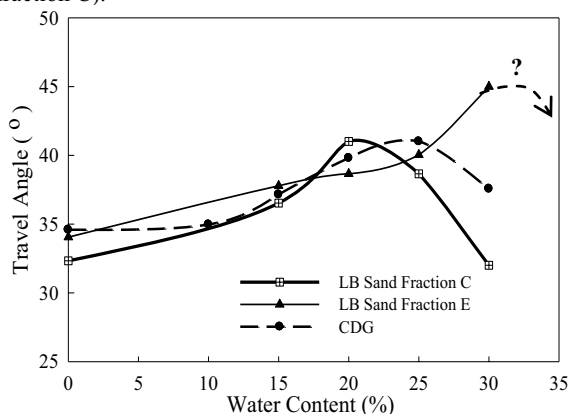


Figure 4. Effects of water content on flow mobility

3.1.2 Effects of total debris mass on flow mobility

Figure 5 compares the measured travel angles of dry CDG and LB sands (fractions C & E) with different flow masses. Similar

linear relationship curves are obtained in the semi-logarithmic coordinate system. These experimental results support and clarify previous research findings that increasing the debris volume (or the mass) generally results in a reduction in the travel angle (Lo 2000). The effect of changing the flowing mass on the variation in the travel angle is similar to descriptions of landslides in the literature.

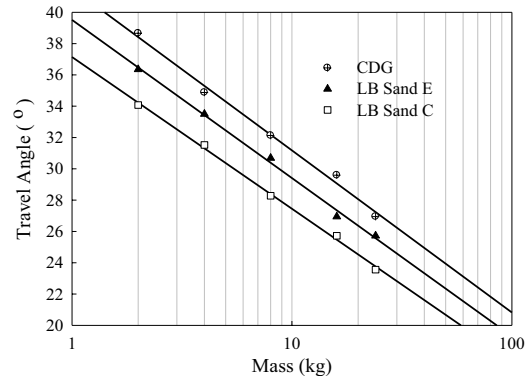


Figure 5. Effect of initial debris mass on flow mobility

3.1.3 Effects of grain size on flow mobility

Figure 6 shows the measured travel angles of flowing materials consisting of different mixtures of dry LB sands (fractions C & E) (see Table 1). The mass of the soil mixture used in each test was 10 kg. The travel angle of dry LB sand (fraction C) was around 26° . An increase in the percentage of fraction E (fine sand) results in an increase in the travel angle. This means that fine particles in granular bodies can reduce the flow mobility.

In granular bodies, a solid particle flowing down along a slope is driven by its gravity, G . The solid particle contacts (shearing) or collides with its neighbouring particles frequently and dissipates the kinetic energy. Obviously, the driving force, G , is proportional to d^3 (d is the particle diameter), and the resistance force, f , acting on the particle surface is proportional to the surface area (i.e., $f \propto d^2$). Then, the ratio of resistance to the driving force, f/G , depends on $1/d$ and governs the flow mobility. Compared to the fine sand flow (fraction E), the f/G ratio for coarse sand flow (fraction C) is relatively small. This implies greater mobility for coarse sand flows in the figure. When the total flowing mass is kept constant, an increase in the percentage of fine particles reduces the mean particle diameter, d , of the granular bodies. This promotes interactions between the particles. Thus, the resulting increase in energy loss reduces the mobility of dry granular flows.

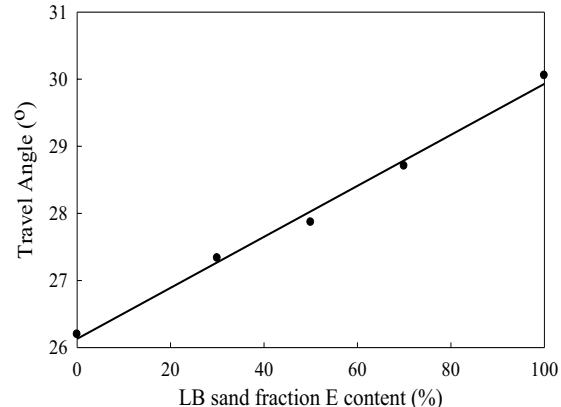


Figure 6. Effects of the proportion of LB sand fraction E on the travel angle

3.2 Study of reverse segregation at the deposition zone

Figure 7 shows the process of deposition in dry CDG particles before hitting a rigid barrier. In the figure, T is time, which is taken to be zero when the debris impacts the barrier. Particle trajectories were captured and the deposition process may be divided into two stages. In the first stage, particle bouncing and collisions are dominant. Coarse particles fall faster and impact the rigid barrier first. Then, they rebound and are buried in the body of the following finer particles. Strong interactions occur between particles. Cracks in the coarse particles are observed, and a cloud of fines is formed (see Figure 7a). Coarse particles are squeezed to the upside while fine particles are squeezed into the inner body (Figure 7b and Figure 7c). Run-up in front of the barrier is observed (Figure 7a to Figure 7c).

In the second stage, after reaching a certain run-up height, the subsequent descending particles slam into and flow over the previously deposited CDG (see Figure 7d). Fine particles in the moving layer penetrate through voids into the bottom layer, with the coarse particles remaining on the free surface. The length of deposited CDG is elongated (Figure 7e). Finally after the deposition process, a sectional view in Figure 7f shows the reverse segregation of dry CDG. The dashed line is the boundary: coarse particles accumulate in the top layer while the fine grains move to the bottom layer. Particle movement in the two stages suggests that both mechanical and geometrical effects are involved in the deposition process. Although Bagnold (1954) attempted to use a dispersive stress mechanism and Middleton (1970) used kinetic sieving to explain the mechanisms of reverse segregation. It is evident that this is not a simple process which can be explained easily.

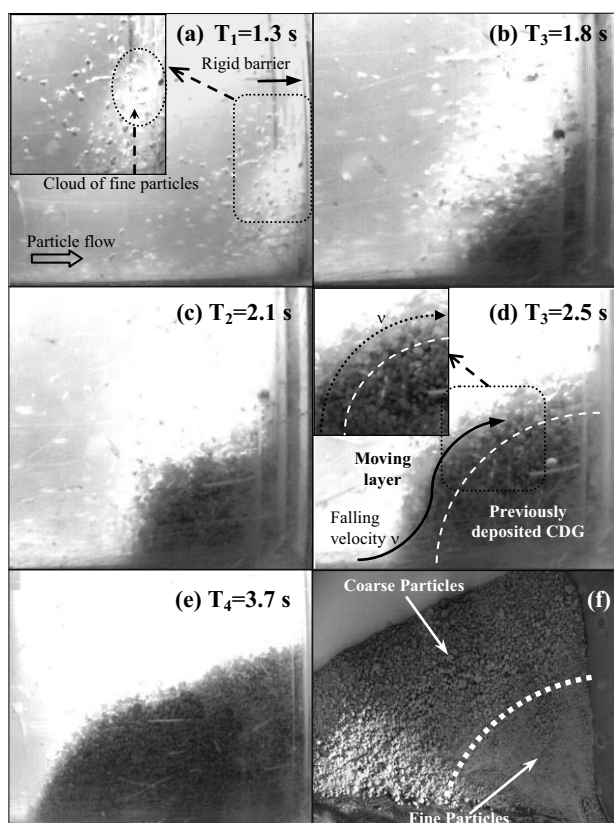


Figure 7. The process of deposition in dry CDG

4 CONCLUSIONS

Based on the physical flume tests, the following conclusions are drawn:

- (1) The mobility of debris flows is significantly influenced by the initial water content. A critical water content exists for flowing granular materials.
- (2) An increase in the total flowing mass in dry granular debris flows corresponds to a reduction in the travel angle (an increase in the flow mobility). Similar phenomenon was observed in different types of granular material.
- (3) The fine particle content can significantly influence the mobility of dry granular flows. The measured travel angle increases as the proportion of fine particles increases.
- (4) Reverse segregation occurs in the deposition of dry granular debris flows. Strong collisions between solid particles are observed before a rigid barrier. Coarse particles are squeezed upwards, while fine particles penetrate through voids and concentrate in the bottom layer. It is evident that this is not a simple process, which can be explained easily.

ACKNOWLEDGEMENTS

The authors would like to acknowledge financial support from research grants DAG05/06.EG39 and HKUST3/CRF-SF/08 provided by Hong Kong University of Science and Technology (HKUST) and GEL05/06.EG01 by Geotech Engineering Ltd. The assistance and contribution by Messrs T.T.L. Yeung, Y. Kwok & T.H.N. Ho and technicians at the Geotechnical Centrifuge Facility, HKUST are also gratefully acknowledged. In addition, the French translation by Dr. A.C.F. Chiu is highly appreciated.

REFERENCES

- Bagnold, R. A. 1954. Experiments on a Gravity-Free Dispersion of Large Solid Spheres in a Newtonian Fluid under Shear. *Proc. R. Soc. London, Ser. A*, 225, 49-63.
- Cruden, D.M. & Varnes, D.J. 1996. Landslide types and processes. In Turner, A.K. & Schuster, R.L. (ed.), *Landslides: Investigation and Mitigation*. Transportation Research Board Special 247, National Research Council: 36-75.
- Davies, T.R.H. 1982. Spreading of Rock Avalanche Debris by Mechanical Fluidization. *Rock Mechanics* 15: 9-24.
- Hunt, B. 1994. Newtonian fluid mechanics treatment of debris flow and avalanches. *Journal of Hydraulic Engineering, ASCE* 120(12): 1350-1363.
- Iverson, R.M. 1997. The physics of debris flow. *Review of Geophysics* 35: 245-296.
- Iverson, R.M. & LaHusen, R.G. 1989. Dynamic pore-pressure fluctuations in rapid shearing granular materials. *Science* 246: 796-799.
- Jakob, M. & Hungr, O. 2005. *Debris-flow hazards and related phenomena*. Praxis: Springer Berlin Heidelberg.
- Law, R.P.H., Zhou, G.D., Chan, Y.M. & Ng, C.W.W. 2007. Investigation of fundamental mechanics of dry granular debris flow. *Proc. 16th Southeast Asia Geot. Conf. 8-11 May, Malaysia*: 781-786.
- Lo, D.O.K. 2000. Review of natural terrain landslide debris-resisting barrier design. GEO Report No. 104, Geotechnical Engineering Office, Hong Kong Special Administrative Region.
- Major, J. J. 1997. Depositional processes in large-scale debris-flow experiments. *Journal of Geology*, 105(3), 345-366.
- Middleton, G. 1970. Experimental studies related to the problem of flysch sedimentation, *Geol. Assoc. Can. Spec. Pap.*, 7, 253-272.
- Ng, C.W.W. & Menzies, B. 2007. *Advanced Unsaturated Soil Mechanics and Engineering*. Publisher: Taylor & Francis. 687p.
- Rombi, J., Pooley, E.J. & Bowman, E.T. 2006. Factors influencing granular debris flow behavior: An experimental Investigation. *Int. J. of Physical Modelling in Geotechnics* 6(1):379-384.
- Takahashi, T. 1991. *Debris flow*. Rotterdam: Balkema.
- Vanapalli, S.K., Fredlund, D.G., Pufahl, D.E. & Clifton, A.W. 1996. Model for the prediction of shear strength with respect to soil suction. *Canadian Geotechnical Journal* 33: 379-392.
- Wang, G. & Sassa, K. 2003. Pore-pressure generation and movement of rainfall-induced landslides: effects of grain size and fine-particle content. *Engineering Geology* 69: 109-125.